Controlling and utilizing optical forces at the nanoscale with plasmonic antennas

Andrea Lovera and Olivier J. F. Martin
Nanophotonics and Metrology Laboratory, Swiss Federal Institute of Technology Lausanne (EPFL), 1015 Lausanne, Switzerland

ABSTRACT

Plasmonic dipole antennas are powerful optical devices for many applications since they combine a high field enhancement with outstanding tunability of their resonance frequency. The field enhancement, which is mainly localized inside the nanogap between both arms, is strong enough to generate attractive forces for trapping extremely small objects flowing nearby. Furthermore it dramatically enhances their Raman scattering cross-section generating SERS emission. In this publication, we demonstrate how plasmonic antennas provide unique means for bringing analyte directly into hot-spots by merely controlling the optical force generated by the plasmon resonance. This technique is very suitable for immobilizing objects smaller that the diffraction limit and requires a very little power density. In this work, 20nm gold nanoparticles functionalized with Rhodamine 6G are trapped in the gap of nanoantennas fabricated with e-beam lithography on glass substrate. The entire system is integrated into a microfluidic chip with valves and pumps for driving the analyte. The field enhancement is generated by a near-IR laser (λ=808nm) that provides the trapping energy. It is focused on the sample through a total internal reflection (TIRF) objective in dark field configuration with a white light source. The scattered light is collected through the same objective and the spectrum of one single antenna spectrum is recorded and analyzed every second. A trapping event is characterized by a sudden red-shift of the antenna resonance. This way, it is possible to detect the trapping of extremely small objects. The SERS signal produced by a trapped analyte can then be studied by switching from the white light source to a second laser for Raman spectroscopy, while keeping the trapping laser on. The trapping and detection limit of this approach will be discussed in detail.

Keywords: Plasmonic trapping, sensing, plasmonic dipole antenna, surface-enhanced Raman spectroscopy, microfluidics.

1. INTRODUCTION

Localized surface plasmon resonances (LSPRs) are very sensitive to variations of the surrounding refractive index and can be used to detect objects attached or in close contact with the metallic surface where the plasmons are generated[1-3]. Furthermore, thanks to the near-field enhancement generated at the edges of plasmonic structures, a parallel use of Surface-Enhanced Raman Spectroscopy (SERS) is also possible to extract information on the kind of chemical compounds on the surface[1-4]. The two techniques are complementary[5] and can give a quantitative and qualitative analysis of molecules and proteins present in an unknown concentration, even in complex solutions. The great advantage of the combination of this techniques is the high sensitivity in term of signal enhancement and spatial confinement, that brings the detection limit down to single molecule[2, 3]. Recently it has been shown that the localized field enhancement can also be used for optical trapping of nanoparticles and biological materials[6-15]. Such plasmonic tweezers are a powerful tool for studying small objects since they require smaller illumination intensities than those needed for conventional optical trapping[7, 8, 12], multiplexing is furthermore possible without the need of complex optical setups[9]. Thanks to the high field enhancement of dipole nanoantennas, trapping of objects smaller than the diffraction limit has been recently achieved and we have demonstrated the trapping of particles as small as 10nm in the gap of a plasmonic antenna[10]. This technique combined with surface functionalization of NPs with molecules, proteins[14, 15], etc, would allows parallel screening of biological compounds. Dipole antennas can further improve the sensitivity because their resonance peaks can be tuned with the length[16] in order to match the highest Raman enhancement condition for the selected excitation wavelength[17, 18]. Finally, the integration of this plasmonic substrate into a microfluidic chip represents a further step toward the realization of a smart platform for sensing and detection[9] with obvious advantages in terms of economy of scales and automation. The design of such kind of chips is based on the work done by Stephen R. Quake[19]. In this work, we combine plasmonic trapping with Raman spectroscopy and integrate the whole lot into microfluidics.

Optical Trapping and Optical Micromanipulation VIII, edited by Kishan Dholakia, Gabriel C. Spalding,
Proc. of SPIE Vol. 8097, 80971Q · © 2011 SPIE · CCC code: 0277-786X/11/$18 · doi: 10.1117/12.892731

In Section 2 we discuss the detection limit of such a system; the experimental setup and microfluidic integration are described in Sec. 3; results are discussed in Sec. 4 and a conclusion is provided in the last section.

2. DETECTION LIMIT OF PLASMONIC ANTENNAS

Plasmonic dipole antennas are extremely sensitive to variations occurring in their surrounding, especially in the regions where the field is strongly enhanced. When the presence of a particle modifies the local refractive index, the antenna resonance wavelength shifts by a quantity proportional to the particle polarizability. Actually, this shift can be utilized to directly detect trapping events by monitoring the LSPR resonance wavelength of the nanoantenna. This trapping relies on strong gradients of the optical field and is more likely to occur where a strong field gradient is generated, i.e. in the nanogap of the antenna, or eventually at the extremities of the antenna[10].
Since the shift of the antenna resonance wavelength depends on the polarizability of the trapped object, a key question for the detection of trapping event is the relation between this shift and the size and composition of the trapped object. Figure 1(a) shows numerical simulations of the antenna resonance wavelength for different particles trapped in the gap. The calculations are done by surface integral equation method[20] and use a realistic shape antenna with nanoparticles (NPs) of different volumes and materials located in the center of the gap[21]. Plasmonic materials generate a significant shift even for small volumes while the sensitivity for trapped dielectric NPs is much lower.

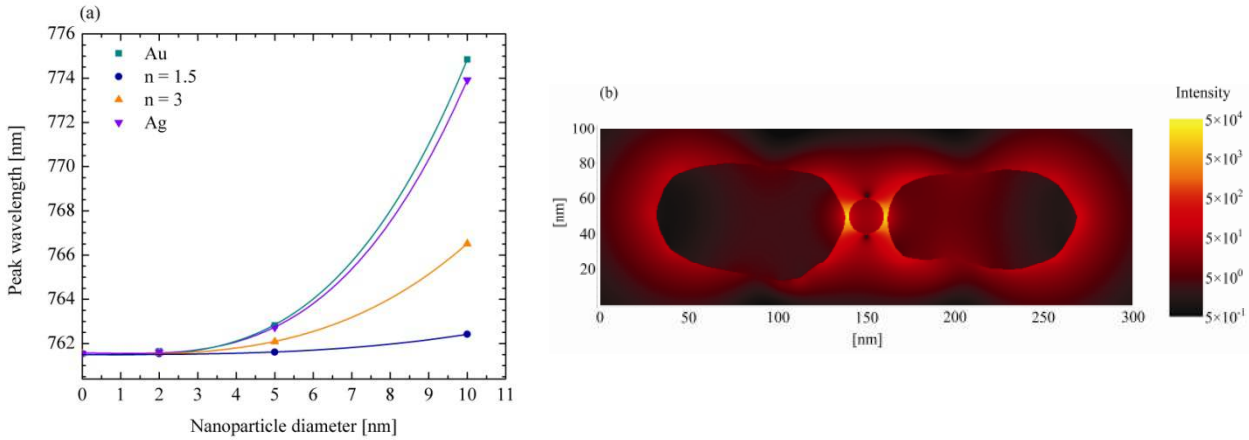

Figure 1. Numerical simulations of a realistic shape antenna with 25nm gap and 105nm length with a NP trapped in the center. (a) The shift of the LSPR caused by the coupling with the NP is plotted as a function of the NP volume and material. (b) Intensity enhancement on a cross-section passing from the center of the structure shows a dramatic improvement of the SERS signal.

Considering a detection limit of our measurement setup of 2nm, it is clear that detecting low refractive index particles as well as very small plasmonic particles remains a challenge. Unfortunately proteins and molecules, which are very relevant experimentally, belong to this category and a different approach must be developed in order to detect them, as detailed in the next section.
Thiol chemistry was used to attach molecules on bare gold NPs that were used as cargo for bringing analytes to the hot spots. They are also much easier to trap due to their higher polarizability and provide much stronger shift in the LSPR. Once the particle is trapped, Raman spectroscopy is used to detect the presence of molecule. This way of detecting biological compound is very powerful since it enables distinguishing among different objects by just comparing their Raman fingerprint. Furthermore, the enhanced field that traps the particles also increases the Raman scattering cross-section and improves by several orders of magnitude the intensity of the signal. This makes the detection of even a few molecules on the NPs possible. Figure 1(b) shows a numerical simulation of a realistic shape antenna with a gold NP in the center of the gap. Its presence contributes to further increase the field enhancement since it creates two tiny gaps at its two extremities. The improvement in the SERS enhancement in this case is very significant.

3. EXPERIMENTAL

2D arrays of gold nanoantennas were fabricated with e-beam lithography and lift-off process keeping width and thickness constant at 40nm. Length and gap size were rather changed respectively along the two axes of the array. The distance between two neighboring antennas was 3.5µm in order to avoid cross-talks during the measurements. Under these conditions single antenna detection is possible. The substrate was then embedded into a two levels microfluidic chip realized in PDMS. The first level contains the actual channels and is in contact with the substrate while the second one, placed on top, serves as driving layer. Crossing channels forming peristaltic pumps and valves were designed to control liquid motion in the main channels using a computer (figure 2). They are actuated by external solenoid valves that turn on and off the pressure inside them closing and opening respectively the channel underneath.

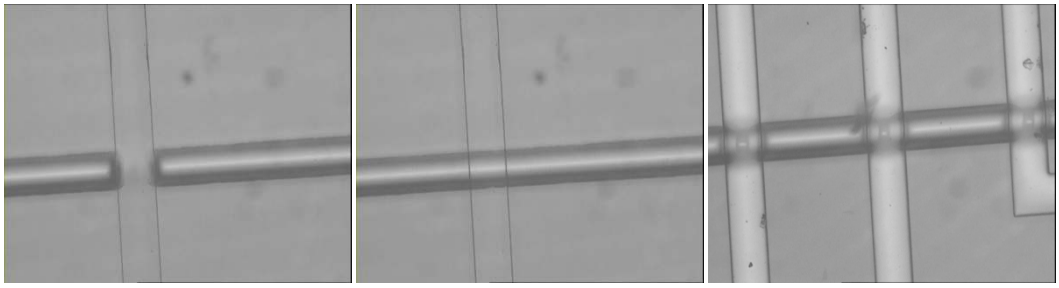

Figure 2. Picture of a close (left) and open (center) channel with the corresponding valve. When the pressure is applied, the upper channel expands and closes the lower one realized in a thin PDMS layer. Example of a peristaltic pump integrated in the chip (right): the peristaltic pump consists in 3 channels that are operated successively to control the liquid motion.

Trapping experiments were performed on an inverted dark-field optical microscope presented in figure 3. The sample was illuminated from the bottom in order to get rid of possible interference with the PDMS microfluidic chip. The trapping energy was provided by a near-IR laser (λ=808nm) impinging on the substrate under total internal reflection and focused on the back plane of the objective in order to achieve diffuse illumination. In this way several antennas were excited in parallel allowing a multiplexed detection. The polarization of the laser was fixed parallel to the antenna length. The read-out was provided by monitoring in real time the LSPR of each antenna by using a white light source. Parallel antennas spectroscopy was achieved by projecting an image of the substrate on the spectrometer slit[22]. A second laser for Raman spectroscopy (λ=632.8nm), was also used for recording the SERS signature coming from each antenna.

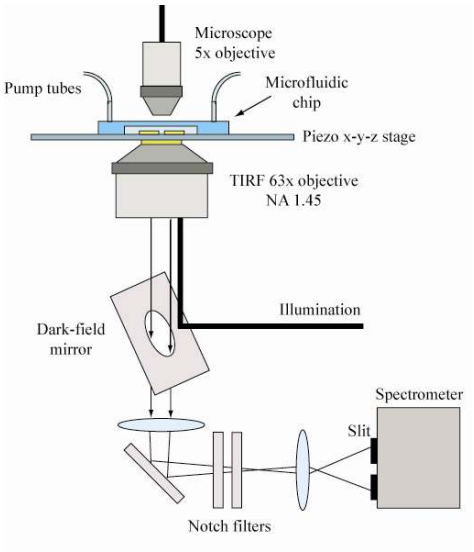

Figure 3. Optofluidic setup: from the top, a standard microscope is used to monitor the microfluidics. The chip is located on a piezo-stage and underneath the dark-field inverted microscope used for the experiments is represented.

NPs were functionalized with ethyl(dimethylaminopropyl)carbodiimide (EDC) chemistry. An excess of Rhodamine 6G modified with two ammine group (Sigma Aldrich) was mixed with polyethylene glycol (PEG) having one thiol group on one end and a carboxylic group on the other end. At the solution were then added EDC and N-hydroxysuccinimide (NHS) in excess, that made the Rhodamine6G and PEG reacting forming a single entity. After 12h gold colloids were added and after further 4h the solution was centrifuged three times in order to remove excess of chemicals. At the end of the process a step of ultrasonication was used to prevent aggregation. The functionalization was monitored by measuring after each step the extinction or scattering spectrum of the solution containing the NPs.

4. RESULTS AND DISCUSSION

Combined trapping and SERS experiments were performed using 20nm gold colloids (Sigma Aldrich) functionalized as explained in Section 3. A halogen lamp and was initially used for monitoring the stability of the resonance of five antennas with same length and different gaps, in water without colloid. Then the NPs were added and the trapping laser switched on. The scattered light from antennas was again collected for 600s with collection time of 0.5s and period of 1s. Figure 4(a) shows the evolution of the plasmon peak in time for an antenna with 25nm gap. After a few seconds a red-shift was recorded while for all the other antennas the peak resonance wavelength was not affected. One can notice that the resonance shift is not abrupt as in the case of bare NPs[10]. A possible explanation for this could be the presence of the molecules that might interact with the walls of the antenna. This aspect has still to be studied in greater details. A minor linear shift was also observed for all antennas; it is probably due to the drift of the substrate on the microscope holder during the experiment. After 600s the lamp was turned off and the Raman laser on. The signal was acquired for 5s and the result is presented in figure 4(b).

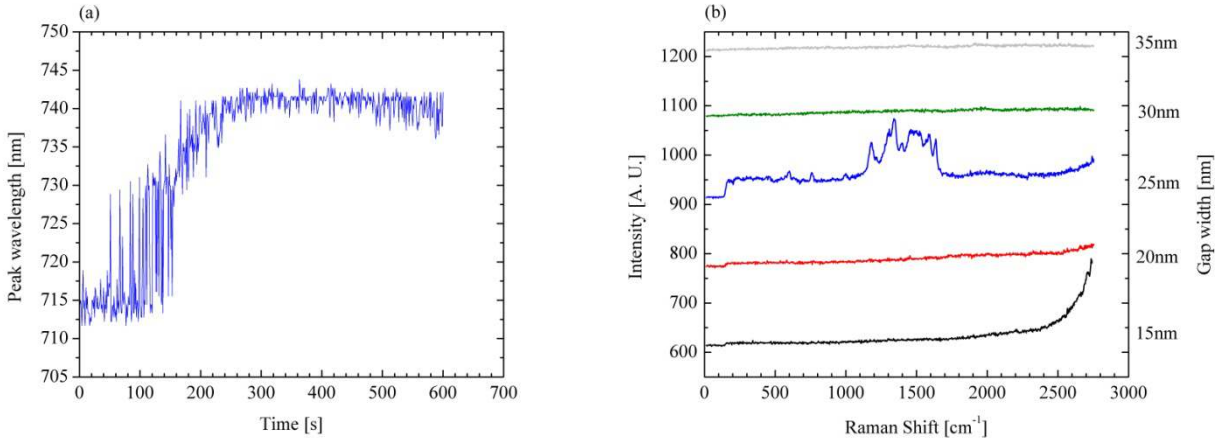

Figure 4. (a) Evolution in time of the plasmon peak wavelength for the 25nm gap antenna with trapping laser on. The red-shift of the resonance is related to the trapping of a NP. (b) Raman signals measured in parallel from the five antennas. The fingerprint of Rhodamine 6G was recorded only from the antenna where the trapping was detected.

A clear fingerprint of Rhodamine 6G was recorded from the antenna with 25nm gap while only a flat background was measured on all the others. After this step, again the scattered light was recorded (figure 5(a)) and the trapping laser switched off. As consequence, the NP in the gap was released and the initial resonance recovered. It can be noticed that before the releasing, a minor red shift was recorded indicated probably a second trapping event. In order to prove that the Rhodamine peaks were generated by the molecules on the particle, Raman signals were again acquired but nothing was recorded, figure 5(b).

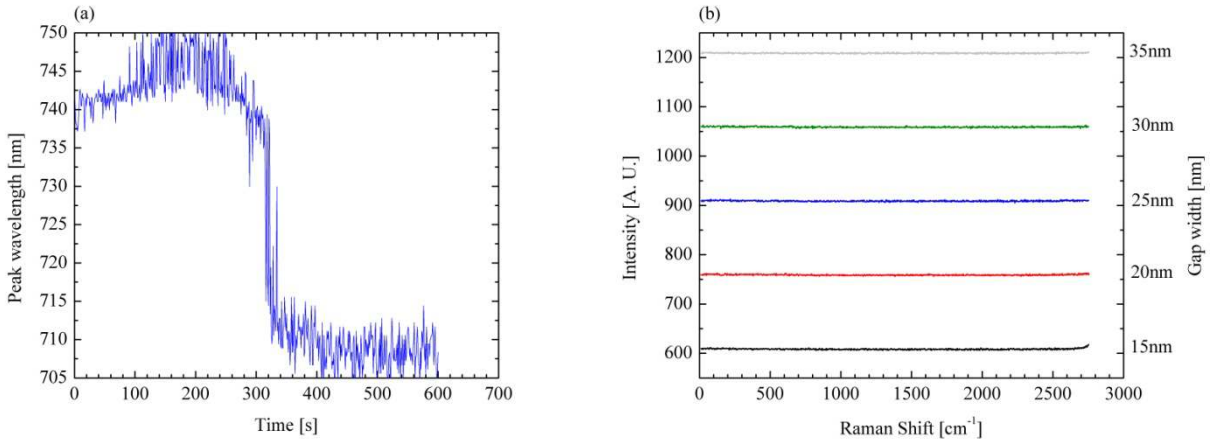

Figure 5. (a) Evolution in time of the plasmon peak wavelength for the 25nm gap antenna. The trapping laser was switched off after 100s. The trapped NP was released after 300s and the resonance came back to the initial value. (b) Raman measurements done after the releasing. None of the antenna generate a SERS signal.

5. SUMMARY

The detection limits for plasmonic trapping was studied using a surface integral approach and realistic shape antennas. The analysis indicates that dielectric particles with low refractive index and plasmonic particle with diameter smaller than 4 nm are difficult to detect directly. A different approach that combines trapping with SERS was developed to overcome this limitation. Functionalized NPs with Rhodamine 6G were first trapped and then the dye was detected with Raman spectroscopy thanks to the high field enhancement of the complex NP-antenna. All the experiments were done in a microfluidic chip. A significant enhancement was observed for the SERS signal. Finally, this technique offers the possibility of parallel detection, since several antenna spectra can be recorded simultaneously.

ACKNOWLEDGEMENT

This work was supported by the European Community's Seventh Framework Program (FP7-ICT-2009-4, Grant agreement 248835).

REFERENCES

[1] Haynes, C. L., C.R., Y., Zhang, X., and Van Duyne, R. P., "Surface-enhanced Raman sensors: early history and the development of sensors for quantitative biowarfare agent and glucose detection," Journal of Raman Specroscopy, 36(6), 471-484 (2005).
[2] Kneipp, K., Wang, Y., Kneipp, H., Perelman, L. T., Itzkan, I., Dasari, R. R., and Feld, M. S., "Single Molecule Detection Using Surface-Enhanced Raman Scattering (SERS)," Physical Review Letters, 78(9), 1667 (1997).
[3] Kneipp, K., and Kneipp, H., "Single Molecule Raman Scattering," Appl. Spectrosc., 60(12), 322A-334A (2006).
[4] Fabris, L., Schierhorn, M., Moskovits, M., and Bazan, G. C., "Aptatag-Based Multiplexed Assay for Protein Detection by Surface-Enhanced Raman Spectroscopy," Small, 6(14), 1550–1557 (2010).
[5] Yonzon, C., Zhang, X., and Van Duyne, R. P., "Localized surface plasmon resonance immunoassay and verification using surface-enhanced Raman spectroscopy," Proceedings of SPIE, 5224, 78-85 (2003).
[6] Righini, M., Zelenina, A. S., Girard, C., and Quidant, R., "Parallel and selective trapping in a patterned plasmonic landscape," Nature Physics, 3, 477-480 (2007).
[7] Righini, M., Volpe, G., Girard, C., Petrov, D., and Quidant, R., "Surface Plasmon Optical Tweezers: Tunable Optical Manipulation in the Femtonewton Range," Phys. Rev. Lett., 100, 186804 (2008).

[8] Righini, M., Ghenuche, P., Cherukulappurath, S., Myroshnychenko, V., Garcia de Abajo, F. J., and Quidant, R., "Nano-optical Trapping of Rayleigh Particles and Escherichia coli Bacteria with Resonant Optical Antennas," Nano Letters, 9(10), 3387–3391 (2009).
[9] Huang, L., Maerkl, S., and Martin, O. J. F., "Integration of plasmonic trapping in a microfluidic environment," Optics Express, 17(8), 6018-6024 (2009).
[10] Zhang, W., Huang, L., Santschi, C., and Martin, O. J. F., "Trapping and Sensing 10 nm Metal Nanoparticles Using Plasmonic Dipole Antennas," Nano Letters, 10(3), 1006-1011 (2010).
[11] Wang, K., Schonbrun, E., Steinvurzel, P., and Crozier, K. B., "Scannable Plasmonic Trapping Using a Gold Stripe," Nano Letters, 10(9), 3506-3511 (2010).
[12] Juan, M. L., Gordon, R., Pang, Y. J., Eftekhari, F., and Quidant, R., "Self-induced back-action optical trapping of dielectric nanoparticles," Nature Physics, 5(12), 915-919 (2009).
[13] Juan, M. L., M., R., and Quidant, R., "Plasmon nano-optical tweezers," Nature Photonics, 5, 349-356 (2011).
[14] Cao, Y., Jin, R., and Mirkin, C. A., "Nanoparticles with Raman Spectroscopic Fingerprints for DNA and RNA Detection," Science, 297, 1536-1540 (2002).
[15] Matschulat, A., Drescher, D., and Kneipp, J., "Surface-Enhanced Raman Scattering Hybrid Nanoprobe Multiplexing and Imaging in Biological Systems," ACS Nano, 4(6), 3259–3269 (2010).
[16] Fischer, H., and Martin, O. J. F., "Engineering the optical response of plasmonic nanoantennas," Opt. Express, 16(12), 9144-9154 (2008).
[17] Haynes, C. L., and Van Duyne, R. P., "Plasmon-Sampled Surface-Enhanced Raman Excitation Spectroscopy," Journal of physical chemistry B, 107, 7426-7433 (2003).
[18] Zhang, W. H., Fischer, H., Schmid, T., Zenobi, R., and Martin, O. J. F., "Mode-selective surface-enhanced Raman spectroscopy usingnanofabricated plasmonic dipole antennas," Journal of Physical Chemistry C, 113(33), 14672-14675 (2009).
[19] Unger, M. A., Chou, H.-P., Thorsen, T., Scherer, A., and Quake, S. R., "Monolithic Microfabricated Valves and Pumps by Multilayer Soft Lithography," Science, 288(113), 113-116 (2000).
[20] Kern, A. M., and Martin, O. J. F., "Surface integral formulation for 3D simulations of plasmonic and high permittivity nanostructures," J. Opt. Soc. Am. A, 26(4), 732--740 (2009).
[21] Kern, A. M., and Martin, O. J. F., "Excitation and Reemission of Molecules near Realistic Plasmonic Nanostructures," Nano Letters, 11(2), 482-487 (2011).
[22] Sonnichsen, C., Geier, S., Hecker, N. E., Plessen, G. v., Feldmann, J., Ditlbacher, H., Lamprecht, B., Krenn, J. R., Aussenegg, F. R., Chan, V. Z. H., Spatz, J. P., and Moller, M., "Spectroscopy of single metallic nanoparticles using total internal reflection microscopy," Appl. Phys. Lett., 77(19), 2949-2951 (2000).